3-2020

Mechanistic Assessment of Functionalized Mesoporous Silica-Mediated Insulin Fibrillation

Mohsen Akbarian

Lobat Tayebi

Soliman Mohammadi-Samani

Fatemeh Farjadian

Journal of Physical Chemistry B, Vol. 124, No. 9 (March 2020): 1637-1652. DOI.

Mechanistic Assessment of Functionalized Mesoporous Silica-Mediated Insulin Fibrillation

Mohsen Akbarian
Pharmaceutical Sciences Research Center, Shiraz University of Medical Sciences, Shiraz 7193371, Iran
Lobat Tayebi
School of Dentistry, Marquette University, Milwaukee, Wisconsin
Soliman Mohammadi-Samani
Pharmaceutical Sciences Research Center, Shiraz University of Medical Sciences, Shiraz 7193371, Iran
Department of Pharmaceutics, Faculty of Pharmacy, Shiraz University of Medical Sciences, Shiraz 7193371, Iran
Fatemeh Farjadian
Pharmaceutical Sciences Research Center, Shiraz University of Medical Sciences, Shiraz 7193371, Iran

ABSTRACT

Insulin, which is a small protein hormone consisting of 51 amino acids, rapidly fibrillates under stressogenic conditions. This biotechnological/ medical problematic reaction quickly accelerates in the presence of some particles, while there are several other particles that slow down the kinetic process.

To address the unexplored demand of the particles that modulate protein fibrillation, we have synthesized two amino-based particles and a chitosan-coated mesoporous silica particle (MS-NH_2, MS-$3NH_2$, and MS-chitosan) to investigate insulin fibrillation. While these particles were fairly similar in size, they are differ in their net positive charge and surface hydrophobicity. To monitor the exact role of the hydrophobic interaction between the protein and MS-chitosan during the fibrillation, we have also co- and preincubated insulin with cholesterol and the particles under stressogenic conditions. The results indicate that MS-NH_2 and MS-$3NH_2$, due to their high positive charges and lack of surface hydrophobicity, repel the positively charged unfolded insulins at pH 2.0. Moreover, MS-chitosan with 25% surface hydrophobicity stacks partially unfolded insulins to its surface and induces some α-helix to β-sheet structural transitions to the protein. Consequently, both amino- and chitosan-based particles slow down the kinetics of the fibrillation. We also showed that cholesterol can structurally participate in insulin fibril architecture as a hydrophobic bridge, and extraction of this molecule from the preformed fibrils may disrupt the fibril structure

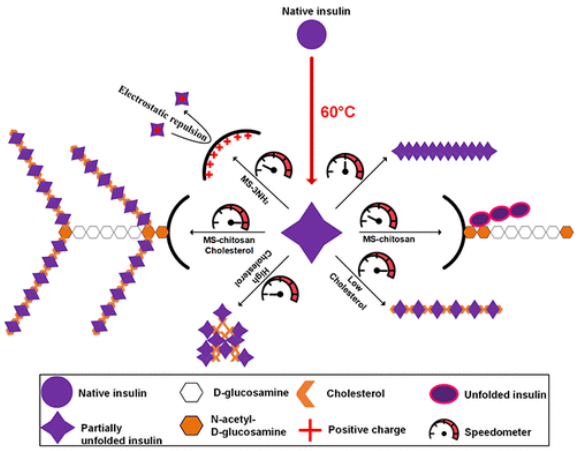

INTRODUCTION

Currently, fibrillations of amyloidogenic proteins are believed to be hallmark characteristics of more than 100 human amyloid diseases. However, from the mechanistic perspective, there is a controversial story behind this process.[1−4] It is generally accepted that amyloid fibrillation is the process in which nontoxic soluble proteins misfold into toxic building blocks, making insoluble and highly protease-resistant fibrils, which contain cross-β-sheet structures.[5,6] It is currently believed that high hydrophobicity, low net charge, and high β-sheet forming propensity are three important factors for partial conversion of the state of a protein into ordered aggregates.[3,7] The protein fibrillation complexity increases further when foreign particles control the kinetics of the reaction.[8,9] Therefore, there is an ongoing debate as to why fibrillation kinetics of the amyloidogenic proteins speed up in the presence of some particles, while the same reaction slows down in the presence of others. Meanwhile, the hydrophobic interactions between particles and protein,[9] as well as the high local concentration of proteins close to particles,8 are accepted as the two main causes improving the rate of protein fibrillation. Moreover, other studies have suggested that the electrostatic interactions between particles and proteins govern the kinetics of the reaction.[10] Another alarming issue is the direct bond

between protein fibrils and particles, which has been investigated before, and likewise, the result has not been satisfactory.[11−13]

A destructive effect of fibrils is their cytotoxicity that may result from the interaction they have with cell membranes.[14,15] According to the obtained evidence, the rate of fibril formation relatively accelerates in the presence of synthetic membrane.[16,17] Among all components present in the cell membrane, researchers have given special attention to cholesterol.[18] Previously, it has been shown that this hydrophobic molecule can attach to protofibrils and fibrils.[19,20] Despite all attempts made to mediate the fibril formation, the results have been inconsistent.[16,21] Yet, there is no clear relationship between cholesterol and fibril formation/cytotoxicity. Nevertheless, important unanswered questions remain, including how foreign particles can modulate the fibrillation rate of a protein.

To address these questions, we have studied three models of functionalized mesoporous silica particles (MS-NH_2, MS-$3NH_2$, and MS-chitosan), varying according to their electrostatic and hydrophobic moieties, on fibrillation of human insulin. Of all the mesoporous materials (particles having a uniform pore size between 2 and 50 nm),[22] mesoporous silica particles, due to their uniform pore size, highly ordered structure, and functionalizability, are of particular interest in industrial and academic communities as drug delivery systems.[23−25] Currently, new applications of these particles are being introduced.[22,26−32]

Using several biophysical methods, in vitro, we have studied mechanisms through which the model particles are able to interact with insulin monomers temporarily to inhibit the fibrillation process. Our particles, in a controlled size, allow us to systematically investigate their possible consequences on the fibrillation. In addition to minimizing the crowding effect between bulk particles and insulin monomers, the selected large size of the particles yields more distinctive results in case the particles and insulin fibrils are directly bound.

Our results show that, unlike MS-chitosan, there are no direct bonds among MS-NH_2, MS-$3NH_2$, and insulin during fibrillation. We have also found that hydrophobic interactions between insulin and MS-chitosan induce structural changes to insulin, making intermediate species highly resistant to fibrillate. In addition, cholesterol, a hydrophobic molecule, makes a strong hydrophobic bridge between MS-chitosan and temperature-induced partially unfolded insulin. Consequently, the generated fibrils are more localized near the particle. Awareness of the fibrillation pathway in pharmaceutical proteins and peptides, such as insulin, in the presence of foreign particles, along with determination of a mechanism to inhibit the process, can be promising with regard to more effective industrialization of therapeutic proteins and peptides.

EXPERIMENTAL SECTION

Materials

Insulin, thioflavin T (ThT), bis-1-anilino-8- naphthalenesulfonate (bis-ANS), and other chemicals were obtained from Sigma (Aldrich, USA). Reverse phase-high performance liquid chromatography (RP-HPLC) solvents and cholesterol were acquired from Caledon Company. Cetyltrimethylammonium bromide (CTAB), tetraethoxysilane (TEOS), and 3-aminopropyl triethoxysilane (APTES) were purchased from Merck Chemical Co. Chitosan/low MW:70 KD, 75% deacetylation was purchased from Sigma-Aldrich. Hydrochloric acid (HCl), ethanol, and acetone were bought from Kimia Mavad (Tehran, Iran).

Preparation of Amino-Mesoporous Silica Particles

On the basis of a previously applied method,[27] MS-NH_2 was prepared. In brief, following dissolution of CTAB (6.6 mmol) in 100 mL of 1:1 deionized water/ethanol solution, 13 mL of ammonia was added to the mixture. During

the 10 min of stirring of the solution at 40 °C, 13.9 mmol of TEOS and 1.5 mmol of APTES were added dropwise to the mixture. The stirring continued for two more hours at 80 °C to produce a white precipitate. After being washed three times in deionized (DI) water and ethanol, the precipitate was dried at 60 °C overnight. Extraction of the surfactant templates was completed using an acidic ethanol (6 mL HCl/200 mL ethanol) solution over 24 h at 90 °C. For preparation of MS-3NH_2, the same procedure was followed, with different amounts of TEOS (10.9 mmol) and APTES (4.5 mmol).

Preparation of Chitosan-Modified Mesoporous Silica Particles

First, the MS-NH_2 synthesis protocol was performed without CTAB removal. After that, for the exterior surface modification, 1 g of this sample was reacted with 0.85 mmol of (3-chloropropyl)triethoxysilane in 100 mL of ethanol for 24 h at 50 °C. Then, CTAB was extracted through a reflux in an acidic ethanol (6 mL HCl/200 mL ethanol) solution for 24 h. The product was filtered and washed according to the previous procedure. Finally, 0.6 g of this product was reacted with chitosan in 30 mL of acetate buffer (pH 5) in the presence of 0.1 g of NaCl for 48 h at 40 °C. The white solid product was filtered and washed with ethanol and acetone, and then dried in a 50 °C oven for 24 h to obtain MS-chitosan.

Kinetics of Monomeric Insulin Fibrillation

The fibrillogenic conditions were selected as 20% acetic acid and pH 2.0 containing 50 mM NaCl in various particle amounts (at 60 °C).[33] Under these conditions, the insulin molecules were present in their monomeric state, and a high temperature was necessary for their partial unfolding, which subsequently promoted insulin to enter the fibrillation pathway.[34] In all cases, insulin was freshly prepared immediately before the experiments, and its concentration was set at 2.0 mg/mL (351 μM) using a molar extinction coefficient of 1.08 (at 276 nm) for 1.0 mg/mL.[35,36] The growth of amyloid fibril was monitored by measuring the ThT fluorescence intensity at 484 nm.[33,37] Upon binding ThT to the fibrils, the positions of excitation and emission maxima moved form 350 and 450 to 450 and 484 nm, respectively.[33,38] Hence, a stock solution of ThT (1.0 mM) was prepared in double-distilled water using a molar extinction coefficient of 24 420 M^{-1} cm^{-1} at 420 nm.[39] The ThT stock solution was kept in the dark at 4 °C before use.

For the in situ ThT fluorescence measurements, 10 μM ThT was added to each protein solution and incubated in a 96 well plate. A total of 150 μL sample volume was added to each well. Also, contributions of different cholesterol concentrations to insulin fibrillation were analyzed in the presence of particles. In all samples, to eliminate the buffer contribution, solutions without protein were prepared, and their spectra were subtracted from the protein spectra. The 484 nm fluorescence intensity was plotted against time, and the kinetic profiles were analyzed by curve fitting using GraphPad Prism V7 (GraphPad Software, Inc. La Jolla, CA, USA). All experiments were performed in triplicate, and finally, average values were presented.

Spectroscopic Analyses

Fluorescence studies were conducted on a Cary Eclipse fluorescence spectrophotometer (Varian Cary Eclipse, USA) equipped with a Peltier unit to control the temperature. All measurements were taken using a 96 black well plate.

Tyr Fluorescence Measurements

To monitor the structural changes of insulin, the intrinsic fluorescence of the protein was monitored by exciting Tyr residues at 276 nm.[40] The fluorescence emission was collected at 280−500 nm. The samples were incubated as previously described.

Measuring the Solvent-Exposed Hydrophobic Surfaces of Insulin Using bis-ANS Dye

The act of binding the fluorophore bis-ANS (final concentration of 10 μM) to insulin samples was studied under fibrillogenic conditions[33,37] in the presence of different cholesterol concentrations and particle amounts. The excitation and emission wavelengths were 350 nm and 400−600 nm, respectively.

Circular Dichroism

The far-UV circular dichroism (CD) spectra were recorded by a Jasco J-810 spectropolarimeter using a cell with a 0.1 mm optical path length at 25 and 60 °C. To analyze α-helix and β-sheet contents of insulin, ellipticities at 209 and 222 nm were recorded.[41,42] Like previous experiments, the insulin concentration was set at 2.0 mg/mL (351 μM).

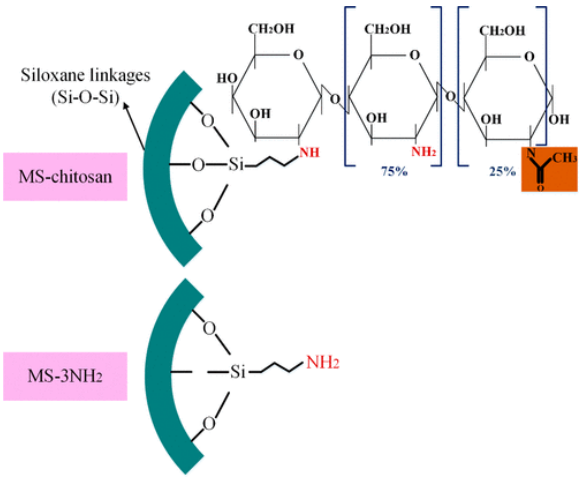

Scheme 1. Illustration of the Particles in This Study

Attenuated Total Reflectance Fourier Transform Infrared Spectroscopy

Attenuated total reflectance Fourier transform infrared (ATR-FTIR) was investigated to trace any reports on the presence of cholesterol in the structure of the fibrils. Therefore, the fibril generated in the absence or presence of cholesterol, as well as cholesterol powder, was prepared and analyzed. A 5.0 mL portion of insulin solution (2.0 mg/mL) in the presence of 2.0 and 4.0 molar ratios of cholesterol-to-insulin was incubated for 6.0 h under the fibrillogenic condition. The generated fibrils were centrifuged (20 min, 13000 g at ambient temperature) and washed three times with methanol/D_2O (MeOH/D_2O) (5.0/95.0, v/v) to remove free cholesterol.[43] To confirm successful washing, after the third wash, using a MeOH/D_2O (5.0/95.0, v/v) blank, the absorbance of the collected supernatant was read at 210 nm to check for the absence of cholesterol. Finally, the fibril samples were washed with pure D_2O to exchange residual methanol by deuterons.41 Finally, the D_2O solutions containing fibrils were spread uniformly on the surface of the attenuated total reflectance (ATR) diamond cell. ATR-FTIR spectra were recorded on a Tensor II instrument (Bruker, Germany) from 1700 to 1600 cm^{-1} (amide I), using a resolution of 2.0 cm^{-1} and an accumulation of 256 scans.[44]

Transmission Electron Microscopic Study

At the end of fibrillation, a 5-fold diluted solution of each sample was deposited on the Formvar carbon-coated copper grids and negatively stained with 1% aqueous uranyl acetate.[45] The specimens were examined at 100 kV excitation voltages with a Philips CM10 transmission electron microscope (Philips, The Netherlands).

Fluorescence Microscopy Imaging

The generated fibrils were mixed with ThT at the final concentration of 50 μM in order to identify the fibrils' cross-connections and lateral interactions. Then, 50 μL of each sample was spread homogeneously onto a

microscopic slide and incubated for 30 min in a dark room.[46] Using excitation/emission filters (469/525 nm), the fluorescence images (Lionheart FX, Bio Tek, USA) were obtained.

Reverse Phase-High Performance Liquid Chromatography

In this study, reverse phase-high performance liquid chromatography (RP-HPLC) was also used to analyze the possible presence of cholesterol in the structure of the fibrils. Similar to FTIR analyses, to remove the free cholesterol, the generated fibrils were washed three times by MeOH/H_2O (5.0/95.0, v/v) at ambient temperature. Then, fibrils were lyophilized (LD Plus Alpha, Christ, Germany) and incubated in acetonitrile/methanol (ACN/MeOH) (50/50, v/v) at 50 °C for 4 h. The supernatant of the samples was obtained by centrifugation (13000 g, 30 min) at ambient temperature. Cholesterol content in the supernatants was quantified using RP-HPLC with a KNAUER HPLC system consisting of a C18 column (ProntoSIL 200-5-C18, 250 mm × 4.6 mm; Apex Scientific) equipped with a UV detector (DAD2, KNAUER). A 20 µL portion of each sample was chromatographed at a flow rate of 1.0 mL/min with an ACN/MeOH (50/50, v/v) solution isocratically, over 25 min at constant temperature (50 °C).[47]

Statistical Analyses

The significance levels were analyzed using one-way ANOVA. The data were analyzed in GraphPad Prism and presented as mean ± SEM. The statistical significance among the groups was determined using analysis of variance, and $P < 0.05$ was considered to be statistically significant.

RESULTS

Choice and Synthesis of the Functionalized Mesoporous Silica Particles

It has been suggested that hydrophobic and electrostatic forces are involved in the interactions between proteins and foreign particles.[9,10] Also, in a previous report, we have shown that induction of positive charges into the insulin primary structure can significantly modulate the protein fibrillation.[48] In the current study, mesoporous silica particles were selected that were functionalized with propylamine and chitosan. The propylamine groups protonate at a relatively low pH, making positively charged particles. Also, depending on the degree of deacetylation in N-acetyl-Dglucosamine, chitosan has a different range of hydrophobic moiety,[49] which allowed the study of the role of this characteristic on human insulin fibrillation (Scheme 1).

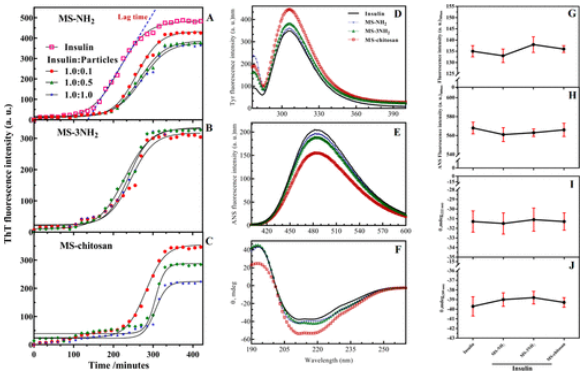

Figure 1. Monitoring the kinetics of insulin fibril formation and structural changes of the protein in the presence of the particles. Insulin fibril formations in the presence of the particles (parts A, B, and C), by ThT fluorescence assessment. Weight ratios of insulin to the particles varied among 1.0:0.1, 1.0:0.5, and 1.0:1.0. (D) The intrinsic tyrosine fluorescence assessment of insulin, (E) the binding ability of insulin to the bis-ANS fluorophore dye, and (F) far-UV CD analyses of the protein at 60 and 25 °C (parts G–J).

Structural Characterization of Applied MS Materials

Three types of MS particles which were utilized in this study were characterized by FTIR spectroscopy, CHN analysis, N2 adsorption/desorption, and an X-ray diffraction technique. The FTIR study (Figure S1) showed the bands attributed to Si−O−Si formation at 1100 cm^{-1} and C−N stretching vibration of propylamine groups that appeared at 1680 cm^{-1} for three types of prepared samples including MS-NH_2, MS-3NH_2, and MS-chitosan. Extra peaks that appeared at approximately 1450 cm^{-1} were attributed to amide groups available in chitosan-coated MS (MS-chitosan). Two types of amino-modified MS species (MS-NH_2 and MS-3NH_2) differed in the number of amino groups. MS-3NH_2 had 3 times more amino groups. CHN analyses were performed to represent the amounts of elements with regard to three types of MS materials (Table S1). The N_2 adsorption/desorption technique through BET calculations showed that MS-NH_2, MS-3NH_2, and MS-chitosan had surface areas of 1085.0766, 270.8607, and 116.2527 m^2 /g. The BJH data attributed to these materials are presented in Table S2. The XRD graph of MS-NH_2 as a representative of mesoporous structure is shown in Figure S2. The particle size distribution of the silica and the protein samples was analyzed by DLS. The hydrodynamic radii of the studied samples are shown in Figure S3. At a glance, as expected, the human insulin sample was found to be in the monomeric and homogeneous state with a size of 1.2 nm when incubated under defined conditions (Figure S3A). For silica particles, the sizes mostly were in the ranges of 334, 289, and 334 nm for MS-NH_2, MS-3NH_2, and MS-chitosan, respectively (Figure S3B−D). Overall, the DLS data suggest that the investigated particles are relatively of the same size. FE-SEM and HR-TEM of MS-NH_2 as representatives of samples were performed, and a typical particle was shown to have a spherical morphology with a size of 183 nm from the FE-SEM (Figure S4A). The HR-TEM image showed a highly ordered mesoporous structure (Figure S4B).

Kinetics of Insulin Fibrillation and Structural Changes of the Protein in the Presence of the Particles and Cholesterol

Human insulin fibrillation was studied in the absence and presence of functionalized MS using an in situ thioflavin T (ThT) binding assay. Generally, as indicated in Figure 1A−C, all three MS particles reduced the rate of insulin fibrillation, while the effect of MS-chitosan was more appreciable. As this figure shows, increasing the amounts of MS-NH_2 and MS-3NH_2 had no significant effect on the kinetics of insulin fibrillation, while, via a concentration-dependent manner, MS-chitosan imposed an inhibiting effect on the process (Table 1).

Table 1. Different Lag Times of Insulin Fibrillation in the Presence of Various Amount of the Particles

		lag time (min)
Insulin		137 ± 7.0
	Insulin:MS-NH_2	
1.0:0.1		194 ± 4.0
1.0:0.5		196 ± 6.0
1.0:1.0		195 ± 7.0
	Insulin:MS-3NH_2	
1.0:0.1		179 ± 9.0
1.0:0.5		156 ± 8.0
1.0:1.0		175 ± 7.0
	Insulin:MS-Chitosan	
1.0:0.1		220 ± 5.0
1.0:0.5		271 ± 6.0
1.0:1.0		268 ± 4.0

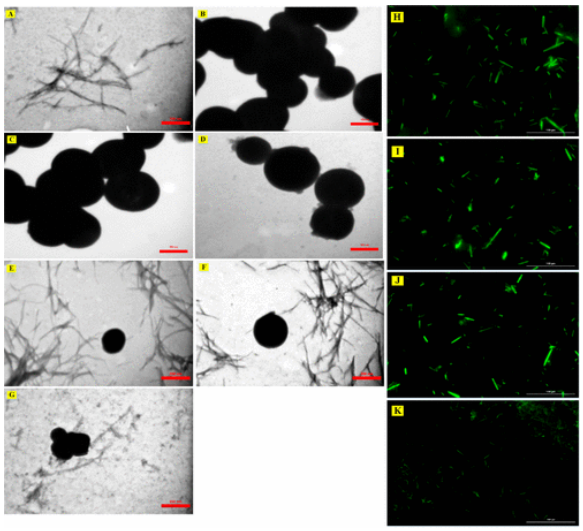

Figure 2. Morphological assessment of the particles and insulin fibrils by transmission electron microscopy. Insulin fibril (A) at the end of fibrillation (420 min). MS-NH_2 (B), MS-3NH_2 (C), and MS-chitosan (D) particles. Fibrillation of insulin in the presence of the MS-NH_2 (E), MS-3NH_2 (F), and MS-chitosan (G). TEM micrographs of the particles are shown with the scale bars of 150 nm, while for other samples imaging was performed by scale bars of 350 nm. Fibril assembly analysis was conducted by fluorescence microscopy (H–K). Assembly and lateral interactions of the mature insulin fibrils in the absence (H), and the presence of MS-NH_2 (I), MS-3NH_2 (J), and MS-chitosan (K) (scale bar 100 µm).

For all cases, in Figure 1A–C, fibrillation kinetics showed typical sigmoidal patterns.[50] Insulin fibrillation kinetics frequently showed a nucleated polymerization process involving three characteristic levels: lag phase, exponential growth phase, and stationary phase. Formation of a critical nucleus occurred in the lag phase, while sizable fibril elongation took place in the growth phase. In the last phase, mature fibrils were formed.[50] Although the particles significantly increased the lag phase of insulin fibrillation, they did not completely inhibit fibril formation of the protein. In the case of the observed ThT intensities, there is still no unanimous agreement on the relationship between the intensity of ThT and the length of fibrils.[38,51] This relationship could be better understood by displaying transmission electron images taken from these samples, which will be discussed later.

In the next section the main focus is the understanding of the attenuating effect of particles, especially MS-chitosan, on the process of insulin fibrillation. In the first step, the structural changes of monomeric insulin in the presence of particles under fibrillogenic conditions were analyzed. To eliminate the crowding effect of the particles and protein, a 1.0:0.1 w/w ratio of insulin to the particles was used in all experiments. The samples were incubated in the predetermined condition for 15 min before the nucleus was generated. Intrinsic fluorescence analyses were used to study structural alterations of the protein (Figure 1A–C). In folded proteins, upon any changes in the protein structure, the intensities of Trp and Tyr fluorophores were checked.[52,53]

Compared to free insulin, MS-NH_2 and MS-3NH_2 did not have any significant effects on the insulin structure, while MS-chitosan increased the Tyr fluorescence intensity notably (Figure 1D). It has been shown that when the nonpolar environment moiety is increased around the Tyr residue, the fluorescence intensity of this amino acid increases as well.[40] To better understand the structural changes in insulin, we also studied the structural differences among the samples by analyzing the bis-ANS binding to the protein. This fluorophore dye has been known to bind to exposed hydrophobic surfaces of the proteins which is useful for analyzing relative conformational changes of the samples.[54]

Similar to intrinsic fluorescence results, the bis-ANS fluorescence intensity increased significantly when MS-chitosan was added. MS-NH_2 and MS-3NH_2 had marginal effects on this characteristic (Figure 1E) indicating the

ignored structural effects of these two particles on insulin integrity. However, in the presence of MS-chitosan, obvious quenching in the bis-ANS intensity occurred. The insulin structure analysis was also conducted through a far-UV CD experiment (Figure 1F). Insulin has been known as a helix rich protein with maximum ellipticity of 209 and 222 nm, while the signals at around 218 nm indicate the β-sheet content of the protein.[55,56] Given these criteria, MS-NH_2 and MS-3NH_2 did not show any appreciable changes in the secondary structure of insulin while MS-chitosan induced some α-helix to β-sheet structural changes along with increasing random coil contents (Figure 1F).

As stated before, all the experiments addressed in Figure 1A−F were conducted at 60 °C. As mentioned earlier, under this condition, insulin underwent some structural changes on its own.[34,57] Thereby, in our system, this altered insulin was able to interact with silica particles. Data presented in Figure 1G−J illustrate alterations of insulin structure in the presence of MS-NH_2, MS-3NH_2, and MS-chitosan at 25 °C. When fluorescence intensities at 305 and 480 nm were recorded in the intrinsic and extrinsic (bis-ANS) fluorescence experiments (Figure 1G,H), no significant structural alterations were observed. A similar experiment was conducted to analyze the changes in the insulin α-helix (Figure 1I,J), and the results were confirmed for limited secondary structural changes of insulin in the presence of all particles at 25 °C. According to the data collected in this study, insulin can undergo more structural alterations in the presence of MS-chitosan if only temperature-induced structural changes occur in the insulin structure itself.

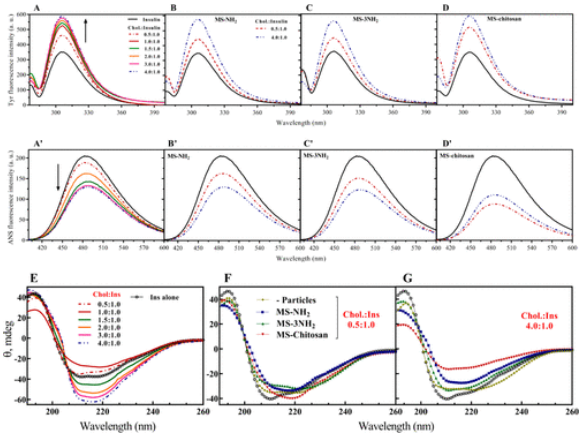

Figure 3. Fibrillation-coupled unfolding of the insulin in the presence of cholesterol detected by Tyr and bis-ANS fluorescences and far-UV CD assessments.

Data from TEM imaging (Figure 2A−G) showed that insulin molecules form fibrils at the end of incubation time. Moreover, in the presence of MS-NH_2 (Figure 2E) and MS-3NH_2 (Figure 2F), preformed insulin fibrils were located far away from these particles, while the fibrils that were generated in the presence of MS-chitosan were very close to it (Figure 2G). Figure 2G also shows that short fibrils were formed in the presence of MS-chitosan.

In the current study, fluorescence microscopy was used to show the bundle of fibrils in the zoom out view.[46] Likewise, the fluorescence microscopic results confirmed the TEM images, indicating a short and slight collection of bundles in the presence of MS-chitosan (Figure 2H−K). Overall, in terms of the delaying effects of all investigated particles on insulin fibrillation, the results from Figures 1 and 2 were astonishing, mainly because MS-NH_2 and MS-3NH_2 had no significant effect on the structure of insulin (Figure 1D−F), and no interaction between these particles and the generated fibrils was observed (Figure 2). More surprisingly, in comparison with those two particles, the MS-chitosan with its somewhat opposite influence had the same effect on insulin fibrillation.

From a chemical point of view, depending on the degree of deacetylation (DD) during chitosan synthesis from chitin, a range of hydrophobic characteristics was considered for this compound.[49] The DD% of chitosan used in this study was ≈75%,[32] and this means that 25 mol % of N-acetyl-Dglucosamine and 75 mol % of D-glucosamine were present. It should be noted that hydrophobic methyl groups in the Nacetyl-D-glucosamine induced the hydrophobic moiety. However, at pH 2.0 (20% acetic acid), free amine groups of chitosan would be protonated and changed to NH_3^+ inducing some positive charges, as indicated by the zeta potential analysis to be 65.4 ± 0.3 mV.

To compare and distinguish the hydrophobic effects exerted on these particles versus those imposed on monomeric insulin during the protein fibrillation, we chose a cholesterol molecule, as a hydrophobic agent, and investigated its effects on this phenomenon.

To analyze the structure alteration of insulin, at first Tyr fluorescence intensity of the protein was studied. Figure 3 shows the structural changes of insulin in the presence of increasing cholesterol-to-insulin molar ratios. By increasing the cholesterol concentrations, the Tyr fluorescence intensity increased gradually. Finally, at 3.0 and 4.0 cholesterol-to-insulin molar ratios, the intensities reached a plateau (Figure 3A). Figure 3B–D shows structural changes of insulin in the presence of particles and two selected cholesterol concentrations (0.5 and 4.0 cholesterol-to-insulin molar ratios). In comparison with cholesterol alone, the results show that there are no significant changes when MS-NH_2 and MS-3NH_2 are separately added to the mixtures containing both 0.5 and 4.0 cholesterol-to-insulin molar ratios (Figure 3B,C). However, in the presence of MS-chitosan and both cholesterol-to-insulin molar ratios, insulin relatively increased the fluorescence intensity (Figure 3D).

Similar experiments were done to analyze the surface hydrophobic area of insulin using bis-ANS dye. Interestingly, though, binding abilities of insulin to bis-ANS reduced when cholesterol concentrations increased in the mixture; this indicates a collapse in the hydrophobic surface areas or these surfaces which are masked by cholesterol (Figure 3A). Like Tyr fluorescence studies, when cholesterol was added in both 0.5 and 4.0 molar ratios, the bis-ANS binding of insulin did not change significantly in the presence of MS-NH_2 and MS-3NH_2, separately (Figure 3B, C). Retrospectively, bis-ANS binding of insulin dramatically reduced in the presence of MS-chitosan in both cholesterol concentrations (Figure 3D).

Insulin structural changes by intrinsic (Tyr) (A−D) and extrinsic (bis-ANS) (A−D) fluorescence studies. Cholesterol-induced secondary structural changes in human insulin in the presence and absence of different particles (E−G).

Further structural analyses were studied using circular dichroism spectroscopy (Figure 3E−G). In the CD study, the α-helix structure was monitored by changes in CD ellipticity at 209 and 222 nm, while the β-sheet structure was traced at 218 nm. Ellipticities under 200 nm were considered as random coil transitions.[42] As indicated in Figure 3E, when the cholesterol-to-insulin molar ratio was increased up to 1.0-fold, both α-helix and β-sheet structures reduced, while the random coil content increased gradually. Interestingly, by increasing this ratio up to 1.5-, 2.0-, 3.0-, and 4.0- folds, β-sheet and random coil transitions to the α-helix content were observed. Insulin in its native state had 58.2% αhelix, 12.4% random coil, and 29.4% β-sheet, as it was deconvoluted here and is in agreement with a previous study.[58] In the presence of a 0.5-fold cholesterol-to-insulin molar ratio, the addition of MS-chitosan dramatically transitioned the α helix and random coil to the β-sheet structure (Figure 3F). In the absence of particles, the only transition observed was that of marginal random coil to α-helix. However, such transitions in the presence of MS-NH_2 and MS-3NH_2 were quite negligible.

Effects of the particles on insulin structural changes in the presence of a 4.0-fold cholesterol-to-insulin molar ratio were also analyzed (Figure 3G). In comparison with Figure 3F, no significant changes were observed in the insulin structure when MS-NH_2 and MS-3NH_2 particles were added. However, in the presence of MS-chitosan, dramatic α-helix and β-sheet transitions to the random coil structure occurred (Figure 3G). Overall, our results

from insulin structure analyses indicate that, in comparison with MS-NH_2 and MS-3NH_2 particles, MS-chitosan is more effective in changing insulin structures in the presence of both cholesterol molar ratios.

Insulin fibrillation was also investigated under the fibrillogenic condition and in the presence of different cholesterol concentrations (Figure 4). In 0.5-, 1.0-, 1.5-, and 2.0-fold cholesterol-to-insulin molar ratios, the lag time of insulin fibrillation reduced gradually (Figure 4A and Table 2). For insulin without cholesterol, ≈136 min lag time was observed, while insulin fibrillations in the presence of 0.5, 1.0, 1.5, and 2.0 cholesterol-to-insulin molar ratios resulted in 91, 31, 20, and 18 min lag times, respectively. Remarkably, the lag time of the fibrillation was considerably prolonged when insulin was incubated with the higher concentration of cholesterol.

As indicated in Figure 4A and Table 2, lag times suddenly shifted to 198 and 256 min in the 3.0 and 4.0 molar ratios of cholesterol-to-insulin, respectively. In this regard study of insulin fibrillation in the presence of the particles and 2.0 and 4.0 molar ratios of cholesterol-to-insulin was investigated. Figure 4B shows that the particles can somewhat attenuate the kinetics of fibrillation, even at a 2.0 molar ratio for cholesterol. This figure implies that there was no significant difference between the lag times related to insulin fibrillation in the presence of the particles when cholesterol was added, while all plots have deviated from the typical sigmoidal pattern and shifted to longer times, due to the presence of a 4.0 molar ratio of cholesterol-to-insulin.

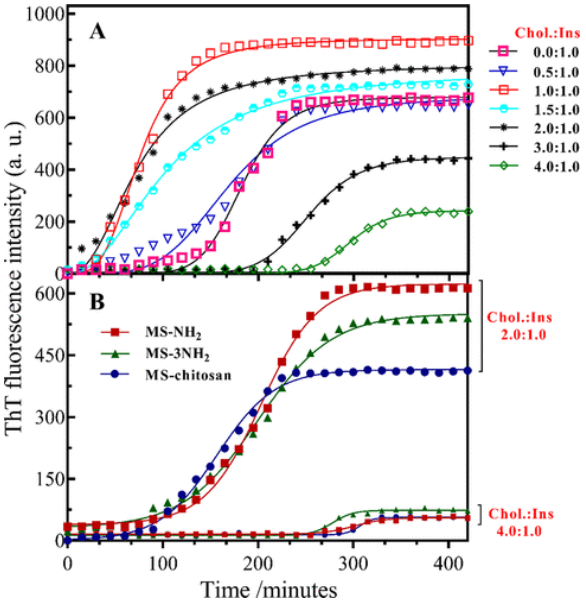

Figure 4. Impact of cholesterol on the kinetics of insulin fibrillation. Insulin (2.0 mg/mL) fibril formation in the presence of different concentrations of cholesterol (at cholesterol-to-insulin molar ratios range 0.5–4.0) (A). The particle-mediated insulin fibrillations at the indicated molar ratios of cholesterol (B). The plots are based on averages of three independent experiments.

Table 2. Lag Times of Insulin Fibrillation in the Presence of Different Concentrations of Cholesterol[a]

insulin:cholesterol (molar ratio)	lag time (min)
1.0:0.0	136 ± 5.0
1.0:0.5	91 ± 4.0
1.0:1.0	31 ± 3.0
1.0:1.5	20 ± 3.0
1.0:2.0	18 ± 4.0
1.0:3.0	198 ± 5.0
1.0:4.0	256 ± 4.0

[a] Insulin concentration was set at 2.0 mg/mL (351 μM).

Morphological assessments of the fibrils were done by TEM (Figure 5A–G). Addition of 0.5 and 2.0 cholesterol-to-insulin molar ratios showed that insulin-formed fibrils are morphologically distinct from those formed in the presence of a molar ratio of 4.0. As shown in Figure 5, the length of fibrils significantly increased under a 2.0 molar ratio of cholesterol-to-insulin in comparison with 0.5 molar ratio. More interestingly, fibril formation in the presence of 4.0 molar ratio was very unusual, both kinetically (Figure 4A) and morphologically (Figure 5). Under this condition, significantly shorter fibrils with the aggregate-like oligomers were observed. As was previously indicated, there were no noteworthy differences between the results obtained from the MS-NH_2- and MS-3NH_2-mediated insulin fibrillation/interaction. Therefore, we decided to continue the study with MS-3NH_2 and MS-chitosan.

As indicated, fibrils formed in the presence of MS-3NH_2 at a 2.0 molar ratio of cholesterol were somewhat far from the particle, while those formed in the presence of MS-chitosan and the same ratio of cholesterol concentration were noticeably closer to the particle. These observations indicate that significant interactions exist between insulin fibrils and MS-chitosan in the absence (Figure 2) and presence (Figure 5) of cholesterol. These two particles were also used for the study of insulin fibrillation at the 4.0 molar ratio of cholesterol (Figure 5F,G). The results of this incubation reveal that, in the presence of MS-3NH_2, the preformed fibrils are obviously short, though, in the presence of MS-chitosan and under defined conditions, insulin sticks to the particle producing an amorphous aggregate.

The fibrils shown in Figure 5A–G were also analyzed by fluorescence microscopy (Figure 5A–G). In agreement with the TEM data, long and sharp plaques of insulin fibrils were observed in the presence of a 2.0 molar ratio of cholesterol-to-insulin, either by adding MS-chitosan or in its absence, whereas aggregated insulin was evident in the 4.0 molar ratio of cholesterol (Figure 5C). More lateral fibril interactions between amorphous aggregates of insulin were exhibited as large fluorescent plaques in all samples with 4.0 molar ratio of cholesterol.

All TEM data obtained from MS-3NH_2-mediated insulin fibrillation indicate that no reliable interactions exist between insulin fibrils and the particle, while MS-chitosan exhibits some interactions with the fibrils in all investigated experiments. Until now, on the basis of the hydrophobic moiety of the chitosan (25% acetylated), we can hypothesize that these interactions between insulin fibrils and the MS-chitosan would be associated with hydrophobic forces of the particle. This hypothesis is evidenced by cholesterol-mediated insulin fibrillation.

We divided the mixtures into three groups including cholesterol + insulin, cholesterol + chitosan, and chitosan + insulin. Each group was incubated for 1 h under stressogenic conditions, and then, the third component and ThT, in appropriate concentrations, were added to the reaction. During this experiment, kinetics of the fibrillation was traced for 420 min (Figure 6). In this experiment, cholesterol was used at 2.0 and 4.0 molar ratios to insulin. In the preincubation of chitosan + cholesterol, the insulin fibrillation rate significantly increased at 2.0 molar ratio of cholesterol, while for a 4.0 molar ratio of cholesterol preincubation, the reaction slowed down. This behavior also resulted in insulin + cholesterol preincubation, while, for the chitosan + insulin treatment, both the 2.0 and 4.0 molar ratios of cholesterol slowed down the rate of fibrillation. Perhaps the most interesting result obtained in this experiment was that the 2.0 molar ratio of cholesterol did not have a noticeable effect on insulin fibrillation when the protein was preincubated with chitosan.

Cholesterol Contribution to the Insulin Fibril Architecture

Following the aforementioned investigations, a unique experiment was conducted to determine the structural participation of cholesterol molecules in the formed insulin fibrils (Figure 7). In this experiment, insulin fibrils which formed in the presence of 2.0 and 4.0 molar ratios of cholesterol were washed in 5% methanol (at 50 °C), and then incubated in ACN/MeOH (50/50, v/v) solution (for details, see the Experimental Section). This solution

was capable of dissolving cholesterol and was also suitable for performing RPHPLC which will be explained later.[47] The pellets containing fibrils were achieved by centrifuging the mixture, and the obtained supernatant was collected for RP-HPLC to study the presence of cholesterol. A similar experiment was also conducted for the insulin fibrils formed in the presence of chitosan at 2.0 and/or 4.0 molar cholesterol ratios. Most interestingly, in comparison with the control insulin fibrils before and after the treatment (Figure 7A,B), the protein fibrils formed in the 2.0 molar ratio of cholesterol were completely broken down after the sample was eluted by ACN/MeOH solution (Figure 7C,D). Also, the treatment of fibrils in this condition led to the daggregation of the amorphous aggregates (Figure 7E,F). In addition, the physical connection between insulin fibrils and MS-chitosan, that was formed in the presence of the 2.0 molar ratio, was thoroughly disrupted after the fibrils were incubated in the ACN/MeOH solution (Figure 7G,H), while at the 4.0 molar ratio, partial broken connections were observed (Figure 7I,J).

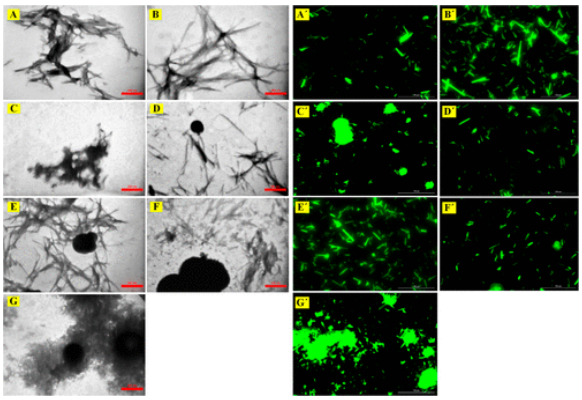

Figure 5. Morphological analyses of insulin fibrils performed in the presence of cholesterol and the particles. TEM micrographs of the insulin fibril in the presence of 0.5 (A), 2.0 (B), and 4.0 (C) cholesterol-to-insulin molar ratios (350 nm scale bars). TEM image of MS-3NH_2 and MS-chitosan at 2.0 (D, E) and 4.0 (F, G) molar cholesterol-to-insulin ratios. Lateral interactions and assemblies of the fibrils in the presence of cholesterol and the particles (A–G).

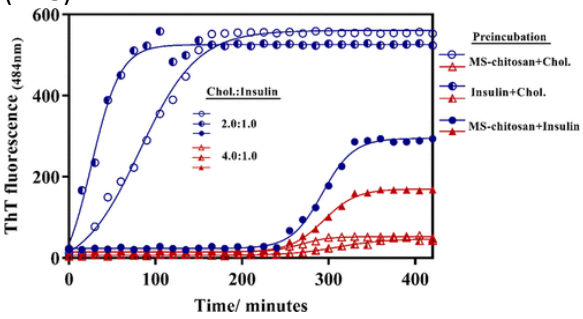

Figure 6. Kinetics of insulin fibrillation at pH 2.0 monitoring by ThT fluorescence assay. Preincubation of MS-chitosan, insulin, and cholesterol at 2.0 and 4.0 molar ratios to insulin, as three groups containing two components, was done for 60 min.

RP-HPLC analyses of obtained supernatants from the previous experiment were used to prove the extraction of the cholesterol from the preformed fibrils during the treatments (Figure 7K–N). In brief, in comparison with a standard cholesterol chromatograph (Figure 7K), all obtained supernatants (Figure 7L–O) had noticeable cholesterol, and these extracted cholesterols were believed to be those which had been dissociated from insulin fibrils structure. This result inspired us to examine the presence of cholesterol in the insulin fibrils by ATR-FTIR spectroscopy. Due to the overlap regarding MS-chitosan and cholesterol FTIR spectra (Figure 8 and Figure S1), this study was conducted for insulin fibrils formed in the cholesterol alone (Figure 8). Figure 8A,B depicts cholesterol and insulin fibrils, respectively. As shown, the FTIR regions corresponding to cholesterol and amide I

were well-evidenced in the formed insulin fibrils at 2.0 and 4.0 molar ratios of cholesterol before the cholesterol was eluted from the fibrils (Figure 8C,D). However, when cholesterol was extracted, the FTIR spectra that corresponded to this molecule were significantly reduced (Figure 8E,F) suggesting the presence of cholesterol molecules in the insulin fibril architecture.

To study the possible interaction between preformed fibrils and cholesterol molecules, postincubation of generated insulin fibrils with the hydrophobic molecule was investigated and morphology of the samples was analyzed by TEM (Figure 9).

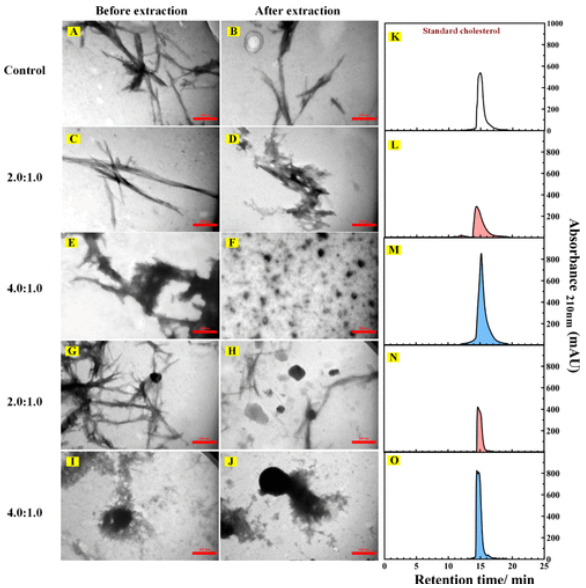

Figure 7. Morphological differences of the formed insulin fibrils after cholesterol is extracted from the fibrils. The TEM micrography was performed for washed (A, C, E, G, and I) and eluted (B, D, F, H, and J) fibrils. In the G, H, I, and J micrographs, the fibrillations were studied in the presence of MS-chitosan. The supernatants that were collected after cholesterol extractions were also analyzed by RP-HPLC assessments (L–O). Standard cholesterol (K) was also eluted in similar methods. The chromatograms were repeated three times. The presented data are the averages of the replicates.

The preformed insulin fibrils were incubated with 2.0:1.0 and 4.0:1.0 molar ratios of cholesterol-to-initial-insulin for 6 h at the stress condition. As seen, no appreciable differences are detected between the samples. This result possibly suggests that the strong cholesterol binding sites in the insulin molecule are most likely the sites where partially unfolded insulin units bind to each other to form mature fibrils. Preferably, cholesterol is able to bind to partially unfolded insulin during the fibrillation process, while fully unfolded insulin which is packed into the fibrils has no visible tendency to bind to the cholesterol molecule. By and large, we observed that cholesterol cannot play a role as a cross-bridge between two or more mature fibrils of insulin, though, from our previous results, it can be concluded that the cholesterol molecules longitudinally participate in the fibril architecture and ubiquitously contribute in insulin amorphous aggregates. This result may also confirm that structures of insulin in the amorphous aggregates and fibrils (morphous aggregates) are considerably different so that a different cholesterol binding affinity has been shown.

DISCUSSION

So far, no common consensus has been achieved regarding the inhibiting or accelerating effects of foreign particles on protein fibrillation.[8,9] However, despite different opinions, it is generally accepted that particles can cause structural changes in proteins as a result of their interaction with the biomacromolecules.[59,60] Also, several

studies have been suggested that particle-mediated protein fibrillation inhibition depends on electrostatic and hydrophobic properties of the particles.[10,61] However, in the current study, we have gained some controversial results.

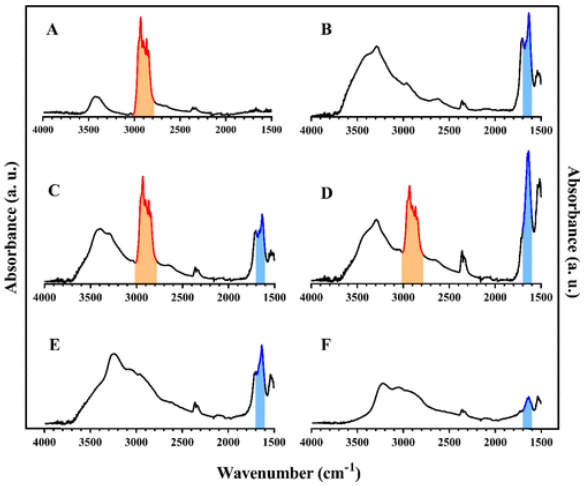

Figure 8. Detection of cholesterol in the structure of insulin fibril by ATR-FTIR. Cholesterol-mediated fibril formation at 2.0 (C, D) and 4.0 (E, F) molar ratios of cholesterol-to-insulin. Pure cholesterol powder (A) and insulin fibril (B) were also analyzed as control samples. Red and blue highlighted parts correspond to possible characteristic peaks for cholesterol and insulin fibril, respectively.

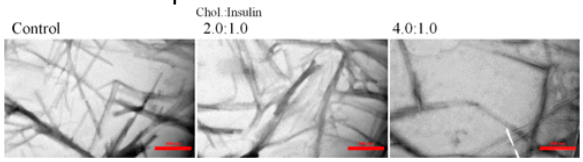

Figure 9. Postincubation of preformed insulin fibrils with two selected cholesterol concentrations.

Our data from Figures 2 and 3 reveal that MS-NH_2 and MS-3NH_2 particles have no significant effect on the monomeric insulin structure, while they are able to slow down the kinetics of insulin fibrillation (Figure 1). In the case of MS-chitosan, all of the data confirm the structural alteration of insulin in the presence of the particle.

Previous studies have confirmed that the monomeric form of insulin undergoes structural changes at the increased temperatures.[34,35] Figure 1 indicates that, among the three different investigated particles, MS-NH_2 and MS-3NH_2 are not able to change insulin structure at either ambient or increased (60 °C) temperatures, while MS-chitosan alters the structure only at 60 °C suggesting an interaction between the MS-chitosan and just partially unfolded insulin.

A previous investigation confirms insulin fibril formation as a hydrophobically and electrostatically driven phenomenon.[33,35,36] On account of 25% acetylated chitosan in this study, among all studied particles, the MS-chitosan has shown a notable hydrophobic characteristic. The hydrophobic propensity of the chitosan has been investigated in several studies, as well.[62,63] Therefore, it was hypothesized that, at 60 °C, insulin undergoes some structural changes, as indicated in our previous work and other studies,[64,65] which induce the formation of aggregation-prone intermediates when exposed to a hydrophobic surface (Figures 2 and 3).

Nevertheless, we have investigated whether the association of insulin fibrils with chitosan is due to hydrophobic interactions. The impact of hydrophobic interactions has been widely examined. Recent clinical studies, related to healthy individuals, have reported elevated plasma cholesterol levels in Alzheimer's disease and type 2 diabetes mellitus.[66,67] In the case of protein amyloid studies, the cholesterol molecule has attracted a lot of attention.[18,19] Others have debated extensively that the cholesterol molecule can not only bind to amyloidogenic

proteins but also interact with other oligomeric states, such as protofibrils and fibrils.[21,68] Our data (Figure 3) also show that the insulin structure changes when cholesterol is added to the solution.

Structurally speaking, insulin has two fibrillation-prone segments, including residues Lys^{B15}, Lys^{B11}, Val^{A3}, Ile^{A2}, Val^{B18}, Leu^{B17}, Tyr^{B16}, Tyr^{B26}, and Ley^{A13} as the hydrophobic segments and Phe^{B1}, Val^{B2}, Asn^{B3}, Gln^{B4}, and His^{B5} segments at the N-terminal B-chain of human insulin.[34] These segments are normally buried in the insulin structure and are only exposed when insulin is partially unfolded. In addition, insulin has four Tyr residues (Tyr^{B26}, Tyr^{B16}, Tyr^{A14}, and Tyr^{A19}).[64] Therefore, two Tyr residues (Tyr^{B26} and Tyr^{B16}) are placed in the hydrophobic segment. We hypothesized that when insulin partially unfolds at 60 °C, the segments will be exposed to the insulin surface. Due to the hydrophobic moiety of these segments and cholesterol molecules, those segments rapidly interact with cholesterol; as a result, an increase in Tyr fluorescence intensity was evident. It is necessary to point out that when Tyr is placed in a hydrophobic environment, its fluorescence intensity increases.40 This also explains the reduced ANS fluorescence intensity. In line with other studies, ANS and the cholesterol molecule seem to compete to interact with the exposed hydrophobic regions of partially unfolded insulin.

On the basis of Figures 6−8, it is inferred that at a 2.0 molar ratio of cholesterol-to-insulin, cholesterol binding to insulin is saturated, and this indicates that two preferable attachment sites exist in the insulin molecule for cholesterol. These sites are most probably those segments that were mentioned before. According to the results, at a 2.0 molar ratio of cholesterol-to-insulin, fibril formation dramatically speeds up, while at the 4.0 molar ratio, the reaction slows down (Figure 4A). Also, investigations of all particles at both 2.0 and 4.0 molar ratios of cholesterol-to-insulin have shown no significant effect on insulin fibrillation. This implies that saturation of insulin by cholesterol does not allow the particles to interact with the protein (Figure 4A).

Figures 5 and 6 consistently show that cholesterol improves the connection between insulin fibril and MS-chitosan at both 2.0 and 4.0 molar ratios (Figure 5E,G). Figure 5D,F indicates that preformed insulin fibrils are far from the particle at 2.0 and 4.0 molar ratios. Therefore, it can be concluded that a hydrophobic interconnection is created between partially unfolded insulins and MS-chitosan by cholesterol which functions as a hydrophobic bridge. A comparison of Figures 4−6 shows that 2.0 molar ratio of cholesterol-to-insulin not only accelerates the rate of fibrillation but also produces long fibrils at the end of the incubation.

According to Figures 1−6, all the data suggest that no interactions are formed between the aminated particles (MS-NH_2 and MS-$3NH_2$) and monomeric insulin. In Figure 6, using preincubation experiments, we have tried to find the order of cholesterol, chitosan, and insulin bindings. On the basis of this result as well as Figures 1 and 3, we suggest that partially unfolded insulins change structurally in the presence of chitosan; hence, these unfolded insulins are not fully able to bind to cholesterol. Also, the bridging function of cholesterol is disturbed in this condition

The structural influence of cholesterol on insulin fibrils is addressed in Figures 3 and 8. As depicted in these figures, a total disruption of the preformed insulin fibril after the treatment suggests that this hydrophobic molecule plays a significant role in the binding of a partially unfolded insulin molecule that leads to the generation of a fibril. Also, detachment of MS-chitosan from insulin fibril shows that cholesterol is a crucial factor in binding these two components. The extraction of cholesterol molecules from the fibril in the collected supernatants is approved by RP-HPLC. In Figure 8, further proof of the presence of cholesterol in the structure of insulin fibrils is presented. An interesting conclusion that can be drawn from the comparison of all the control treatment results (Figures 7A,B and 8A,B) is that interactions between unfolded insulin monomers in the fibrils are notably stronger than interactions between cholesterol and the partially unfolded insulin monomer. As previously indicated, the structure of β2-microglobulin amyloid fibrils in the 80% dimethylsulfoxide is totally dissolved.[69] Also, disassembly of bovine insulin amyloid fibrils results in 70% of the reagent.[70] All the aforementioned results and our study indicate that hydrophobic interactions play an important role in the

process of stacking the building blocks to make fibrils. In our study, the interactions between insulin building blocks are adequately stable, even in the presence of ACN/MeOH (50/50, v/v). Regarding the delayed effects of MS-NH_2 and MS-3NH_2 on the insulin fibrillation, it is suggested that positive charges in the particles as well as in the surface of insulin molecules at pH 2.0 make a repulsive force and repel the partially unfolded insulin. Some previous studies, also, have indicated the importance of electrostatic interactions in the fibril formation.[71,72]

Changes in the strength of the acidity, itself, do not have a significant effect on the structure of insulin55,56 but strongly influence the insulin oligomerization states.[33,48] At acidic conditions, equilibria from hexamers shift to lower oligomers, and in the presence of higher temperatures, the monomeric state would be populated. This observation has been suggested due to protonation of a His^{B10} at the trimer interface.[73] Several studies have been focused on the study of the adsorption mechanism of protein on the surface of nanoparticles. By and large, a strong relationship between degree of particle ionization and protein (or peptide) binding affinity has been suggested.[74−76] In this kind of interaction, the charged residues in the protein, i.e., arginine and lysine, are the main part of the interaction, via H-bond interactions with the particle's surface.[74] In the case of insulin, it should be noticed that the net charge of monomeric human insulin is about +6 near pH 2.0.[50] As shown here, interactions between insulin and charged particles also highly depend on the environmental pH. Consequently, unlike the previous study that has been conducted by other particles, the local concentration of the partially unfolded insulin is dispersed, and this affects the kinetics of fibrillation. It is very important to note that the preformed fibrils at the 4.0 molar ratio are short and slightly distinguishable in the presence of MS-3NH_2 (Figure 5F), while the fibrils are completely aggregated in the presence of MS-chitosan (Figure 5F). This reinforces our hypothesis that, upon the positive repulsion between MS-3NH_2 and positively charged partially unfolded insulins, an aggregate-like oligomer is not generated in the presence of the 4.0 molar ratio. Given the obtained data, a schematic representation is shown here (Scheme 2).

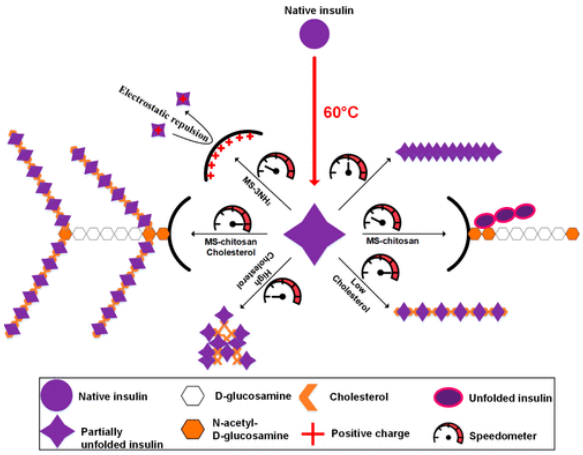

Scheme 2. Summary of the Results Obtained in This Study[a]

[a]Degreed semicircular logo shows speedometer of the corresponded reaction.

In summary, under the acidic environment (20% acetic acid, pH 2.0) and at an elevated temperature (60 °C), insulin hexamers dissociate into partially unfolded monomers, exposing some hydrophobic surface areas. Subsequently, this state of insulin, through hydrophobic interactions, can bind to hydrophobic parts of MS-chitosan. Upon this interaction, some structural characteristics (α-helix to β-sheet transition) transit insulin from fibril-prone species to aggregate-prone intermediates making the protein more resistant to form fibrils (Scheme 2). Meanwhile, in the presence of a low concentration of cholesterol (at 2.0 molar ratio of cholesterol-to-insulin), partially unfolded insulin molecules can best stack to each other, making long and distinguishable fibrils. Also, there is another explanation for this observation; partially unfolded insulin molecules with exposed

hydrophobic patches attach to cholesterol resulting in an increase in the local concentration of insulin near the preformed fibril networks, finally trapping the protein units inside the fibrillar network.

However, this phenomenon can lead to production of slightly disrupted and aggregate-like oligomers in the presence of a high concentration of cholesterol due to the crowding effect of the hydrophobic molecules. As the most interesting result in this study, when insulin fibrillation is investigated in the presence of cholesterol and MS-chitosan, preferentially, cholesterol bonds to chitosan induces a hydrophobic bridge between the particle and partially unfolded protein (Scheme 2). Also, as mentioned before, MS-3NH_2 and MS-NH_2 repel the fibril-prone species of insulin, and this attenuates the fibrillation process.

CONCLUSION

In conclusion, a unique relationship exists between partially hydrophobic particles (MS-chitosan) and insulin fibril formation. It is also proven that hydrophobic small molecules, such as cholesterol, can structurally contribute to the insulin fibril structure. These findings may be of interest in designing suitable particles to preserve pharmaceutical proteins and peptides during downstream processing of the products.

ASSOCIATED CONTENT

Supporting Information

The Supporting Information is available free of charge at https://pubs.acs.org/doi/10.1021/acs.jpcb.9b10980. Characterization of the structural features of the MS-NH_2 and MS-3NH_2 and MS-chitosan particles using CHN elemental analyses, the surface area and volume measurements, FTIR assessments, DLS analyses, X-ray diffraction pattern, and representative FE-SEM and HRTEM images for MS-NH_2 (PDF)

AUTHOR INFORMATION

Corresponding Author

Fatemeh Farjadian − Pharmaceutical Sciences Research Center, Shiraz University of Medical Sciences, Shiraz 7193371, Iran; orcid.org/0000-0002-2093-0454; Phone: +987132424127(302); Email: farjadian_f@ sums.ac.ir; Fax: +987132424126

Authors

Mohsen Akbarian − Pharmaceutical Sciences Research Center, Shiraz University of Medical Sciences, Shiraz 7193371, Iran

Lobat Tayebi − School of Dentistry, Marquette University, Milwaukee, Wisconsin 53233-2186, United States

Soliman Mohammadi-Samani − Pharmaceutical Sciences Research Center and Department of Pharmaceutics, Faculty of Pharmacy, Shiraz University of Medical Sciences, Shiraz 7193371, Iran

Complete contact information is available at: https://pubs.acs.org/10.1021/acs.jpcb.9b10980

Funding

This work was supported by the Research Council of Shiraz University of Medical Sciences (Grant 98-01-36-20502).

Notes

The authors declare no competing financial interest.

ACKNOWLEDGMENTS

The authors would like to thank the Research Council of Shiraz University of Medical Sciences for supporting this project under Grant 98-01-36-20502. Also, the authors wish to thank Mr. H. Argasi at the Research Consultation Center (RCC) of Shiraz University of Medical Sciences for his invaluable assistance with language editing for this manuscript.

REFERENCES

(1) Furukawa, Y.; Kaneko, K.; Matsumoto, G.; Kurosawa, M.; Nukina, N. Cross-seeding fibrillation of Q/N-rich proteins offers new pathomechanism of polyglutamine diseases. J. Neurosci. 2009, 29 (16), 5153−5162.
(2) Yagi, H.; Kusaka, E.; Hongo, K.; Mizobata, T.; Kawata, Y. Amyloid Fibril Formation of α-Synuclein Is Accelerated by Preformed Amyloid Seeds of Other Proteins implications for the mechanism of transmissible conformational diseases. J. Biol. Chem. 2005, 280 (46), 38609−38616.
(3) Bhasikuttan, A. C.; Mohanty, J. Detection, inhibition and disintegration of amyloid fibrils: the role of optical probes and macrocyclic receptors. Chem. Commun. 2017, 53 (19), 2789−2809.
(4) Shinde, M. N.; Barooah, N.; Bhasikuttan, A. C.; Mohanty, J. Inhibition and disintegration of insulin amyloid fibrils: a facile supramolecular strategy with p-sulfonatocalixarenes. Chem. Commun. 2016, 52 (14), 2992−2995.
(5) Nielsen, L.; Frokjaer, S.; Brange, J.; Uversky, V. N.; Fink, A. L. Probing the mechanism of insulin fibril formation with insulin mutants. Biochemistry 2001, 40 (28), 8397−8409.
(6) Huang, K.; Maiti, N. C.; Phillips, N. B.; Carey, P. R.; Weiss, M. A. Structure-specific effects of protein topology on cross-β assembly: studies of insulin fibrillation. Biochemistry 2006, 45 (34), 10278− 10293.
(7) Chiti, F.; Stefani, M.; Taddei, N.; Ramponi, G.; Dobson, C. M. Rationalization of the effects of mutations on peptide andprotein aggregation rates. Nature 2003, 424 (6950), 805.
(8) Colvin, V. L.; Kulinowski, K. M. Nanoparticles as catalysts for protein fibrillation. Proc. Natl. Acad. Sci. U. S. A. 2007, 104 (21), 8679−8680.
(9) Linse, S.; Cabaleiro-Lago, C.; Xue, W.-F.; Lynch, I.; Lindman, S.; Thulin, E.; Radford, S. E.; Dawson, K. A. Nucleation of protein fibrillation by nanoparticles. Proc. Natl. Acad. Sci. U. S. A. 2007, 104 (21), 8691−8696.
(10) Mohammad-Beigi, H.; Hosseini, A.; Adeli, M.; Ejtehadi, M. R.; Christiansen, G.; Sahin, C.; Tu, Z.; Tavakol, M.; Dilmaghani-Marand, A.; Nabipour, I.; et al. Mechanistic Understanding of the Interactions between Nano-Objects with Different Surface Properties and αSynuclein. ACS Nano 2019, 13 (3), 3243−3256.
(11) Cabaleiro-Lago, C.; Szczepankiewicz, O.; Linse, S. The effect of nanoparticles on amyloid aggregation depends on the protein stability and intrinsic aggregation rate. Langmuir 2012, 28 (3), 1852−1857.
(12) Zeng, H.-j.; Miao, M.; Liu, Z.; Yang, R.; Qu, L.-b. Effect of nitrogen-doped graphene quantum dots on the fibrillation of hen eggwhite lysozyme. Int. J. Biol. Macromol. 2017, 95, 856−861.
(13) Zhao, L.; Xin, Y.; Li, Y.; Yang, X.; Luo, L.; Meng, F. Ultraeffective Inhibition of Amyloid Fibril Assembly by Nanobody− Gold Nanoparticle Conjugates. Bioconjugate Chem. 2019, 30 (1), 29− 33.
(14) Stefani, M. Biochemical and biophysical features of both oligomer/fibril and cell membrane in amyloid cytotoxicity. FEBS J. 2010, 277 (22), 4602−4613.
(15) Engel, M. F.; Khemtemourian, L.; Kleijer, C. C.; Meeldijk, H.́ J.; Jacobs, J.; Verkleij, A. J.; de Kruijff, B.; Killian, J. A.; Höppener, J. W. Membrane damage by human islet amyloid polypeptide through fibril growth at the membrane. Proc. Natl. Acad. Sci. U. S. A. 2008, 105 (16), 6033−6038.
(16) Cheng, B.; Li, Y.; Ma, L.; Wang, Z.; Petersen, R. B.; Zheng, L.; Chen, Y.; Huang, K. Interaction between amyloidogenic proteins and biomembranes in protein misfolding diseases: mechanisms, contributors, and therapy. Biochim. Biophys. Acta, Biomembr. 2018, 1860 (9), 1876−1888.

(17)Terakawa, M. S.; Yagi, H.; Adachi, M.; Lee, Y.-H.; Goto, Y. Small liposomes accelerate the fibrillation of amyloid β (1−40). J. Biol. Chem. 2015, 290 (2), 815−826.
(18)Kakio, A.; Nishimoto, S.-i.; Yanagisawa, K.; Kozutsumi, Y.; Matsuzaki, K. Cholesterol-dependent formation of GM1 gangliosidebound amyloid β-protein, an endogenous seed for Alzheimer amyloid. J. Biol. Chem. 2001, 276 (27), 24985−24990.
(19)Drolle, E.; Gaikwad, R. M.; Leonenko, Z. Nanoscale electrostatic domains in cholesterol-laden lipid membranes create a target for amyloid binding. Biophys. J. 2012, 103 (4), L27−L29.
(20)Dong, X.; Qiao, Q.; Qian, Z.; Wei, G. Recent computational studies of membrane interaction and disruption of human islet amyloid polypeptide: Monomers, oligomers and protofibrils. Biochim. Biophys. Acta, Biomembr. 2018, 1860 (9), 1826−1839.
(21)Niu, Z.; Zhang, Z.; Zhao, W.; Yang, J. Interactions between amyloid β peptide and lipid membranes. Biochim. Biophys. Acta, Biomembr. 2018, 1860 (9), 1663−1669.
(22)Farjadian, F.; Roointan, A.; Mohammadi-Samani, S.; Hosseini, M. Mesoporous silica nanoparticles: Synthesis, pharmaceutical applications, biodistribution, and biosafety assessment. Chem. Eng. J. 2019, 359, 684−705.
(23)Pal, N.; Bhaumik, A. Soft templating strategies for the synthesis of mesoporous materials: Inorganic, organic−inorganic hybrid and purely organic solids. Adv. Colloid Interface Sci. 2013, 189, 21−41.
(24)Liu, P.; Chen, G.-F. Porous Materials: Processing and Applications; Elsevier, 2014.
(25)Farjadian, F.; Ghasemi, A.; Gohari, O.; Roointan, A.; Karimi, M.; Hamblin, M. R. Nanopharmaceuticals and nanomedicines currently on the market: challenges and opportunities. Nanomedicine 2019, 14 (1), 93−126.
(26)Farjadian, F.; Ahmadpour, P.; Samani, S. M.; Hosseini, M. Controlled size synthesis and application of nanosphere MCM-41 as potent adsorber of drugs: a novel approach to new antidote agent for intoxication. Microporous Mesoporous Mater. 2015, 213, 30−39.
(27)Farjadian, F.; Ghasemi, S.; Heidari, R.; Mohammadi-Samani, S. In vitro and in vivo assessment of EDTA-modified silica nano-spheres with supreme capacity of iron capture as a novel antidote agent. Nanomedicine 2017, 13 (2), 745−753.
(28)Taqanaki, E. R.; Heidari, R.; Monfared, M.; Tayebi, L.; Azadi, A.; Farjadian, F. EDTA-modified mesoporous silica as supra adsorbent of copper ions with novel approach as an antidote agent in copper toxicity. Int. J. Nanomed. 2019, 14, 7781−7792.
(29)Farjadian, F.; Ghasemi, S.; Mohammadi-Samani, S. Hydroxylmodified magnetite nanoparticles as novel carrier for delivery of methotrexate. Int. J. Pharm. 2016, 504 (1−2), 110−116.
(30)Farjadian, F.; Azadi, S.; Mohammadi-Samani, S.; Ashrafi, H.; Azadi, A. A novel approach to the application of hexagonal mesoporous silica in solid-phase extraction of drugs. Heliyon 2018, 4 (11), No. e00930.
(31)Heidarinasab, A.; Ahmad Panahi, H. A.; Faramarzi, M.; Farjadian, F. Synthesis of thermosensitive magnetic nanocarrier for controlled sorafenib delivery. Mater. Sci. Eng., C 2016, 67, 42−50.
(32)Farjadian, F.; Moradi, S.; Hosseini, M. Thin chitosan films containing super-paramagnetic nanoparticles with contrasting capability in magnetic resonance imaging. J. Mater. Sci.: Mater. Med. 2017, 28 (3), 47.
(33)Ahmad, A.; Uversky, V. N.; Hong, D.; Fink, A. L. Early events in the fibrillation of monomeric insulin. J. Biol. Chem. 2005, 280 (52), 42669−42675.
(34)Brange, J.; Andersen, L.; Laursen, E. D.; Meyn, G.; Rasmussen, E. Toward understanding insulin fibrillation. J. Pharm. Sci. 1997, 86 (5), 517−525.
(35)Ahmad, A.; Millett, I. S.; Doniach, S.; Uversky, V. N.; Fink, A. L. Partially folded intermediates in insulin fibrillation. Biochemistry 2003, 42 (39), 11404−11416.
(36)Ahmad, A.; Millett, I. S.; Doniach, S.; Uversky, V. N.; Fink, A. L. Stimulation of insulin fibrillation by urea-induced intermediates. J. Biol. Chem. 2004, 279 (15), 14999−15013.

(37)Hong, D.-P.; Ahmad, A.; Fink, A. L. Fibrillation of human insulin A and B chains. Biochemistry 2006, 45 (30), 9342−9353.
(38)Khurana, R.; Coleman, C.; Ionescu-Zanetti, C.; Carter, S. A.; Krishna, V.; Grover, R. K.; Roy, R.; Singh, S. Mechanism of thioflavin T binding to amyloid fibrils. J. Struct. Biol. 2005, 151 (3), 229−238.
(39)Muzaffar, M.; Ahmad, A. The mechanism of enhanced insulin amyloid fibril formation by NaCl is better explained by a conformational change model. PLoS One 2011, 6 (11), No. e27906.
(40)Bekard, I. B.; Dunstan, D. E. Tyrosine autofluorescence as a measure of bovine insulin fibrillation. Biophys. J. 2009, 97 (9), 2521− 2531.
(41)Bouchard, M.; Zurdo, J.; Nettleton, E. J.; Dobson, C. M.; Robinson, C. V. Formation of insulin amyloid fibrils followed by FTIR simultaneously with CD and electron microscopy. Protein Sci. 2000, 9 (10), 1960−1967.
(42)Kelly, S. M.; Jess, T. J.; Price, N. C. How to study proteins by circular dichroism. Biochim. Biophys. Acta, Proteins Proteomics 2005, 1751 (2), 119−139.
(43)Stadtman, T. C. [63] Preparation and assay of cholesterol and ergosterol. Methods Enzymol. 1957, 3, 392.
(44)Zako, T.; Sakono, M.; Hashimoto, N.; Ihara, M.; Maeda, M. Bovine insulin filaments induced by reducing disulfide bonds show a different morphology, secondary structure, and cell toxicity from intact insulin amyloid fibrils. Biophys. J. 2009, 96 (8), 3331−3340.
(45)Hong, D.-P.; Fink, A. L. Independent heterologous fibrillation of insulin and its B-chain peptide. Biochemistry 2005, 44 (50), 16701− 16709.
(46)Santhoshkumar, P.; Raju, M.; Sharma, K. K. αA-Crystallin peptide 66SDRDKFVIFLDVKHF80 accumulating in aging lens impairs the function of α-Crystallin and induces lens protein aggregation. PLoS One 2011, 6 (4), No. e19291.
(47)Gilk, S. D.; Cockrell, D. C.; Luterbach, C.; Hansen, B.; Knodler, L A.; Ibarra, J. A.; Steele-Mortimer, O.; Heinzen, R. A. Bacterial colonization of host cells in the absence of cholesterol. PLoS Pathog. 2013, 9 (1), No. e1003107.
(48)Akbarian, M.; Yousefi, R.; Moosavi-Movahedi, A. A.; Ahmad, A.; Uversky, V. N. Modulating insulin fibrillation using engineered Bchains with mutated C-termini. Biophys. J. 2019, 117 (9), 1626−1641.
(49)Lee, D. W.; Lim, C.; Israelachvili, J. N.; Hwang, D. S. Strong adhesion and cohesion of chitosan in aqueous solutions. Langmuir 2013, 29 (46), 14222−14229.
(50)Groenning, M.; Frokjaer, S.; Vestergaard, B. Formation mechanism of insulin fibrils and structural aspects of the insulin fibrillation process. Curr. Protein Pept. Sci. 2009, 10 (5), 509−528.
(51)Meehan, S.; Knowles, T. P.; Baldwin, A. J.; Smith, J. F.; Squires, A. M.; Clements, P.; Treweek, T. M.; Ecroyd, H.; Tartaglia, G. G.; Vendruscolo, M.; et al. Characterisation of amyloid fibril formation by small heat-shock chaperone proteins human αA-, αB-and R120G αBcrystallins. J. Mol. Biol. 2007, 372 (2), 470−484.
(52)Chan, F. T.; Kaminski Schierle, G. S. K.; Kumita, J. R.; Bertoncini, C. W.; Dobson, C. M.; Kaminski, C. F. Protein amyloids develop an intrinsic fluorescence signature during aggregation. Analyst 2013, 138 (7), 2156−2162.
(53)Biophysical and Biochemical Aspects of Fluorescence Spectroscopy; Dewey, T. G., Ed.; Springer, 1991.
(54)Datki, Z.; Olah, Z.; Macsai, L.; Pakaski, M.; Galik, B.; Mihaly, G.; Kalman, J. Application of BisANS fluorescent dye for developing a novel protein assay. PLoS One 2019, 14 (4), No. e0215863.
(55)Hua, Q.-x.; Weiss, M. A. Mechanism of insulin fibrillation the structure of insulin under amyloidogenic conditions resembles a protein-folding intermediate. J. Biol. Chem. 2004, 279 (20), 21449− 21460.
(56)Hua, Q. Insulin: a small protein with a long journey. Protein Cell 2010, 1 (6), 537−551.

(57)Nielsen, L.; Khurana, R.; Coats, A.; Frokjaer, S.; Brange, J.; Vyas, S.; Uversky, V. N.; Fink, A. L. Effect of environmental factors on the kinetics of insulin fibril formation: elucidation of the molecular mechanism. Biochemistry 2001, 40 (20), 6036−6046.
(58)Li, Y.; Huang, L.; Yang, X.; Wang, C.; Sun, Y.; Gong, H.; Liu, Y.; Zheng, L.; Huang, K. The effect of exposing a critical hydrophobic patch on amyloidogenicity and fibril structure of insulin. Biochem. Biophys. Res. Commun. 2013, 440 (1), 56−61.
(59)Fei, L.; Perrett, S. Effect of nanoparticles on protein folding and fibrillogenesis. Int. J. Mol. Sci. 2009, 10 (2), 646−655.
(60)Lynch, I.; Dawson, K. A. Protein-nanoparticle interactions. Nano Today 2008, 3 (1−2), 40−47.
(61)Asthana, S.; Hazarika, Z.; Nayak, P. S.; Roy, J.; Jha, A. N.; Mallick, B.; Jha, S. Insulin adsorption onto zinc oxide nanoparticle mediates conformational rearrangement into amyloid-prone structure with enhanced cytotoxic propensity. Biochim. Biophys. Acta, Gen. Subj. 2019, 1863 (1), 153−166.
(62)Amiji, M. M. Pyrene fluorescence study of chitosan selfassociation in aqueous solution. Carbohydr. Polym. 1995, 26 (3), 211−213.
(63)Philippova, O. E.; Volkov, E. V.; Sitnikova, N. L.; Khokhlov, A. R.; Desbrieres, J.; Rinaudo, M. Two types of hydrophobic aggregates in aqueous solutions of chitosan and its hydrophobic derivative. Biomacromolecules 2001, 2 (2), 483−490.
(64)Akbarian, M.; Ghasemi, Y.; Uversky, V. N.; Yousefi, R. Chemical modifications of insulin: Finding a compromise between stability and pharmaceutical performance. Int. J. Pharm. 2018, 547 (1−2), 450−468.
(65)Akbarian, M.; Yousefi, R. Human αB-Crystallin as fusion protein and molecular chaperone increases the expression and folding efficiency of recombinant insulin. PLoS One 2018, 13 (10), No. e0206169.
(66)Whiley, L.; Sen, A.; Heaton, J.; Proitsi, P.; García-Gomez, D.; Leung, R.; Smith, N.; Thambisetty, M.; Kloszewska, I.; Mecocci, P.; et al. Evidence of altered phosphatidylcholine metabolism in Alzheimer's disease. Neurobiol. Aging 2014, 35 (2), 271−278.
(67)Zhang, M.; Zhou, J.; Liu, Y.; Sun, X.; Luo, X.; Han, C.; Zhang, L.; Wang, B.; Ren, Y.; Zhao, Y.; et al. Risk of type 2 diabetes mellitus associated with plasma lipid levels: The rural Chinese cohort study. Diabetes Res. Clin. Pract. 2018, 135, 150−157.
(68)Harris, J. R. Cholesterol binding to amyloid-β fibrils: A TEM study. Micron 2008, 39 (8), 1192−1196.
(69)Hirota-Nakaoka, N.; Hasegawa, K.; Naiki, H.; Goto, Y. Dissolution of β2-microglobulin amyloid fibrils by dimethylsulfoxide. J. Biochem. 2003, 134 (1), 159−164.
(70)Zhang, G.; Babenko, V.; Dzwolak, W.; Keiderling, T. A. Dimethyl sulfoxide induced destabilization and disassembly of various structural variants of insulin fibrils monitored by vibrational circular dichroism. Biochemistry 2015, 54 (49), 7193−7202.
(71)Xu, Y.; Claiden, P.; Zhu, Y.; Morita, H.; Hanagata, N. Effect of amino groups of mesoporous silica nanoparticles on CpG oligodexynucleotide delivery. Sci. Technol. Adv. Mater. 2015, 16 (4), 045006.
(72)Guo, M.; Gorman, P. M.; Rico, M.; Chakrabartty, A.; Laurents, D. V. Charge substitution shows that repulsive electrostatic interactions impede the oligomerization of Alzheimer amyloid peptides. FEBS Lett. 2005, 579 (17), 3574−3578.
(73)Whittingham, J. L.; Scott, D. J.; Chance, K.; Wilson, A.; Finch, J.; Brange, J.; Dodson, G. G. Insulin at pH 2: structural analysis of the conditions promoting insulin fibre formation. J. Mol. Biol. 2002, 318 (2), 479−490.
(74)Grasso, G.; Mercuri, S.; Danani, A.; Deriu, M. A. Biofunctionalization of Silica Nanoparticles with Cell Penetrating Peptides: Adsorption Mechanism and Binding Energy Estimation. J. Phys. Chem. B 2019, 123, 10622.
(75)Sprenger, K.; Pfaendtner, J. Strong electrostatic interactions lead to entropically favorable binding of peptides to charged surfaces. Langmuir 2016, 32 (22), 5690−5701.

(76)Konno, T. Amyloid-Induced Aggregation and Precipitation of Soluble Proteins: An Electrostatic Contribution of the Alzheimer's β (25− 35) Amyloid Fibril. Biochemistry 2001, 40 (7), 2148−2154.